Genetics and Molecular Research

Isolation and characterization of a novel acidic matrix protein hic22 from the nacreous layer of the freshwater mussel, *Hyriopsis cumingii*

X.J. Liu[1]*, C. Jin[1]*, L.M. Wu[1], S.J. Dong[1], S.M. Zeng[1] and J.L. Li[1,2]

[1]Key Laboratory of Freshwater Aquatic Genetic Resources, Shanghai Ocean University, Ministry of Agriculture, Shanghai, China
[2]E-Institute of Shanghai Universities, Shanghai Ocean University, Shanghai, China

*These authors contributed equally to this study.
Corresponding author: J.L. Li
E-mail: jlli2009@126.com

Genet. Mol. Res. 15 (3): gmr.15038656
Received March 24, 2016
Accepted June 2, 2016
Published July 29, 2016
DOI http://dx.doi.org/10.4238/gmr.15038656

ABSTRACT. Matrix proteins that either weakly acidic or unusually highly acidic have important roles in shell biomineralization. In this study, we have identified and characterized hic22, a weakly acidic matrix protein, from the nacreous layer of *Hyriopsis cumingii*. Total protein was extracted from the nacre using 5 M EDTA and hic22 was purified using a DEAE-sepharose column. The N-terminal amino acid sequence of hic22 was determined and the complete cDNA encoding hic22 was cloned and sequenced by rapid amplification of cDNA ends-polymerase chain reaction. Finally, the localization and distribution of hic22 was determined by *in situ* hybridization. Our results revealed that

hic22 encodes a 22-kDa protein composed of 185 amino acids. Tissue expression analysis and *in situ* hybridization indicated that hic22 is expressed in the dorsal epithelial cells of the mantle pallial; moreover, significant expression levels of hic22 were observed after the early formation of the pearl sac (days 19-77), implying that hic22 may play an important role in biomineralization of the nacreous layer.

Key words: Freshwater mussel; *Hyriopsis cumingii*; Nacre; Matrix protein; Biomineralization

INTRODUCTION

Biomineralization is a biological process by which living organisms produce various minerals using environmental elements that are selectively precipitated on specific organic matter (Veis, 1981). Mollusk shells are common biological minerals. Matrix proteins and other biological macromolecules, such as glycoproteins, lipids, and polysaccharides, are involved in the formation of the nacreous and prismatic layers of mollusk shells. Although matrix proteins account for only 5% (w/w) of the mineralized layer, they can regulate crystal nucleation, morphology, growth, and orientation with nanoscale precision (Sarikaya and Aksay, 1992; Addadi et al., 2006). As a result, the shell has a unique structure and excellent mechanical properties at the nano-level; this indicates that matrix proteins play a decisive role in guiding shell formation (Alivisatos, 2000). Dozens of individual matrix proteins have been isolated since the extraction of the first matrix protein conchiolin from the shell by Fremy, advancing research into nacre formation (Kono et al., 2000; Miyashita et al., 2000; Norizuki and Samata, 2008). However, the mechanisms underlying nacre formation are complicated and difficult to analyze; therefore, several additional matrix proteins must be isolated and characterized to better explain the process.

The pearl aquaculture industry has developed rapidly over the past few years; however, this has been accompanied by a reduction in the quality of pearls, which has caused serious problems. *Hyriopsis cumingii* is the most important mussel species utilized for freshwater pearl production in China. Statistically, 70% of all freshwater pearls are produced by this species (Bai et al., 2014). Therefore, research into nacre formation could help improve the yield and quality of pearls.

The prismatic and nacreous layers of *H. cumingii* shells are made of aragonite (Liu and Li, 2015). Several studies have been conducted on the organic matrix to explore the mechanism of biomineralization (Ma et al., 2010, 2011). The acid-soluble matrix of the vaterite pearl reportedly induces the crystallization of vaterite, while the water-soluble matrix of aragonite pearls facilitates the production of aragonite crystals (Ma et al., 2012). Moreover, a comparison of the microstructure and composition of aragonite and vaterite pearls with the nacre layer of *H. cumingii* shells revealed that vaterite tablets are packed with a greater number of organic matrices and exhibited a more irregular texture compared to that of aragonite tablets (Ma et al., 2013). A 48-kDa acidic and putative calcium-binding glycoprotein, believed to affect crystal growth, was isolated and characterized from *H. cumingii* pearls (Natoli et al., 2010). The recently cloned nacrein gene reportedly codes for a protein that could accelerate the growth of prismatic-shaped crystals by influencing the secretion of mantle tissue (Han et al., 2010). Perlucin is another important matrix protein of *H. cumingii* that is believed to induce pearl

formation (Lin et al., 2013). Studies into the recently cloned *HcCS1* gene have demonstrated its important role in shell formation via the regulation of chitin synthesis (Zheng et al., 2015). Silkmapin is another new matrix protein that has been shown to participate in the nucleation of calcium carbonate, providing nucleation sites to facilitate nacre formation (Liu et al., 2015). However, a limited number of studies have been conducted on individual matrix proteins. In this study, a gene encoding a shell matrix protein (named hic22) was isolated from the *H. cumingii* cDNA library and subjected to quantitative real-time PCR (qRT-PCR) and *in situ* hybridization. These analyses indicated that hic22 may play a role in nacre biomineralization.

MATERIAL AND METHODS

Samples

Twenty *H. cumingii* were collected from the Wuyi pearl farm (Jinhua, Zhejiang Province, China). The mussels were cultured in the river-way for 5 days before the experiment to avoid a stress reaction. The nacre protein matrix was extracted from the shells of 20 individuals (shell length: 7.5-8.0 cm) and the RNA was extracted from the tissues and pearl sacs of 300 *H. cumingii* individuals.

Extraction of total protein from the nacre

The shells were cleaned and immersed in 5% NaOH for 10 h to remove the organic components and contaminants on the shell surface; subsequently, the prismatic layer was mechanically cleaned in a drying state. The nacre was powdered (50 g) and suspended in 100 mL 5 M EDTA solution for 12 h at 4°C with continuous stirring. Total nacre protein was collected by centrifuging the supernatant at 15,000 *g* for 40 min at 4°C and subjecting the product to ultrafiltration in a Merck ultrafiltration tube (Merck, Kenilworth, NJ, USA).

Protein purification and N-terminal sequencing

Nacre total protein was loaded onto a DEAE-Sepharose column (2 x 10 cm) equilibrated with 25 mM Tris-HCl, pH 7.4. The column was washed with 25 mM Tris-HCl, pH 7.4, until a baseline absorbance of 220 nm was achieved; the column was then eluted with a linear gradient of 0.0-0.5 M NaCl in Tris-HCl. The eluate was collected every 3 min, and measured at an absorbance of 220 nm. The major peak fractions (0.3 M NaCl) were pooled and analyzed by sodium dodecyl sulfate polyacrylamide gel electrophoresis (SDS-PAGE). The hic22-containing eluates were pooled and dialyzed against Milli-Q water, and concentrated by ultrafiltration (Millipore ultrafiltration tube; cutoff 5 kDa). The N-terminal sequence was determined by blotting the 22-kDa band obtained from SDS-PAGE on to a polyvinylidene difluoride (PVDF) filter (Millipore) using a blotting system (BioRad, Hercules, CA, USA). The band was then cut off and analyzed using the LF3000 amino acid sequence analyzer (Beckman-Coulter, Brea, CA, USA).

RNA extraction from tissues and pearl sacs

Tissues were removed from the adductor muscle, foot, intestine, mantle pallial,

mantle edge, gill, and hemocyte and stored in RNAstore (Tiangen, Beijing, China) at -80°C. Five oysters were randomly harvested on days 3, 6, 9, 12, 19, 23, 26, 29, 33, 45, and 77 post-implantation. The pearl sac in the mantle tissue of these oysters was carefully peeled off and immediately stored in RNAstore (Tiangen). Total RNA was extracted using Trizol (Thermo Fisher Scientific, Waltham, MA, USA) according to the manufacturer instructions. The RNA quality was determined by electrophoresing on a 1.5% agarose gel, and its concentration was determined by NanoDrop (Thermo Fisher Scientific) analysis.

Rapid amplification of cDNA ends (RACE) and bioinformatic analysis

The full-length cDNA of hic22 was synthesized using a Smart RACE amplification kit (Clontech, Mountain View, CA, USA) and Advantage 2 cDNA polymerase mix (Clontech). A degenerate primer Hic22-F1 (5'-CTNAAYGAYACNATYCCNGCNCTN-3'; N = A/G/C/T, Y = C/T) was designed based on the N-terminal sequence for 3'-RACE. The gene-specific antisense primer Hic22-R1 (5'-ACAGATACTCACATCACCG-3') was designed for 5'-RACE based on the cDNA fragment designed by 3'-RACE. Homogenous proteins were searched using GenBank, SwissProt, and Basic Local Alignment Search Tool (BLAST). The open reading frame (ORF) of *hic22* cDNA was determined by an ORF Finder (http://www.ncbi.nlm.nih.gov/projects/gorf/), and the signal peptide was analyzed using the SignalP 4.1 server (http://www.cbs.dtu.dk/services/SignalP/). The secondary structure of the protein was predicted by Phyre2 (http://www.sbg.bio.ic.ac.uk/phyre/).

Gene expression analysis

Total RNA was isolated from different tissues and pearl sacs and reverse transcribed into cDNA for qRT-PCR using the Reverse Transcriptase kit (Promega, Madison, WI, USA) according to the manufacturer protocols. The hic22-specific primers Hic22-F2 (5'-CGCCACTACACTCATAGACAA-3') and Hic22-R2 (5'-GGACACGAAAGAACTACAC AAC-3') were designed for qRT-PCR. EF-1α was used as the internal standard. qRT-PCR was performed in a 20-μL reaction mixture, comprising 10 μL SYBR FAST Master mix (Takara Bio Inc., Otsu, Japan), 0.4 μL primer (10 μM each), 1 μL cDNA (12 μM), and 8.2 μL RNase-free water. The qRT-PCR conditions were set as follows: initial denaturation at 95°C for 3 min; 39 cycles of denaturation at 95°C for 10 s and annealing at 60°C for 30 s. The threshold cycle (CT) of each sample was measured using the Mx3000P software. The relative expression level of *hic22* in different tissues and pearl sacs was calculated using the $2^{-\Delta\Delta Ct}$ equation.

In situ hybridization

A hic22 DNA fragment was cloned to synthesize the digoxigenin (DIG)-labeled RNA probes. The recombinant vector was transformed to competent DH5α cells, which were cultured overnight on Luria-Bertani agar plates at 37°C. The positive clones were propagated and the plasmids were extracted. DIG-labeled RNA probes were synthesized from the linearized plasmid using a standard DIG RNA labeling kit (Roche Diagnostics, Basel, Switzerland). The SP6 and T7 RNA polymerases (Takara Bio Inc., Otsu, Japan) were used to synthesize the sense and antisense probes, respectively.

The mantle tissue was collected and soaked in 4% (w/v) paraformaldehyde for 6 h

and incubated with 20% sucrose buffer at 4°C for 20 h until the tissue sank to the bottom. The tissue blocks were cut into uneven sections (10-mm increments) with a freezing microtome (Leica, Wetzlar, Germany). *In situ* hybridization was performed using the Enhanced Sensitive ISH Detection kit (Boster, Wuhan, China) according to manufacturer protocols.

RESULTS

Hic22 purification

Total nacre protein was loaded onto a DEAE-sepharose column, and the major peak fractions were eluted using 0.3 M NaCl (Figure 1). The purified hic22 was detected by SDS-PAGE (Figure 2). Only one band was visualized at 22 kDa and the band was blotted onto a PVDF filter for N-terminal sequencing. A peptide with the amino acid sequence "LNDTIPALNATIPES" was identified, and a 3'-RACE primer was designed based on this N-terminal sequence.

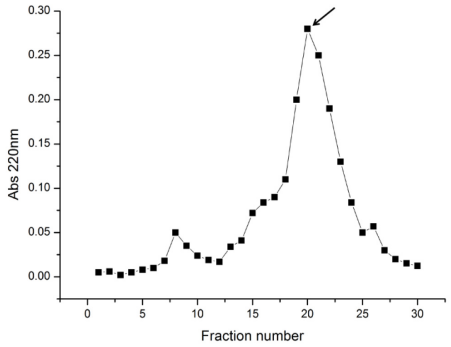

Figure 1. Elution profile of total protein extracted from the nacreous layer. The eluate consisted of a linear gradient of 0-0.5 M NaCl. The arrow is pointing to hic22.

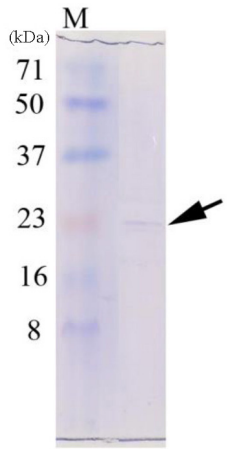

Figure 2. SDS-PAGE of hic22 purified from the nacreous layer. The arrow is pointing to hic22.

cDNA cloning and sequence analysis

A 615-bp fragment was amplified by 3'-RACE, and a 309-bp fragment was amplified by 5'-RACE. A 731-bp cDNA sequence was obtained by piecing these fragments together (Figure 3). hic22 contained a 621-bp ORF encoding a sequence containing 206 amino acids, with a theoretical molecular weight of 22.51 kDa and an estimated isoelectric point of 5.60. A signal peptide was predicted from residues 1-21 (Figure 3). The theoretical molecular weight and isoelectric point of the sequence excluding the signal peptide were 17.57 kDa and 6.03, respectively. The predicted secondary structure of hic22 was mainly composed of two α-helical regions and two β-sheet regions; the β-sheets were predicted to be located between the two α-helix regions (Figure 4).

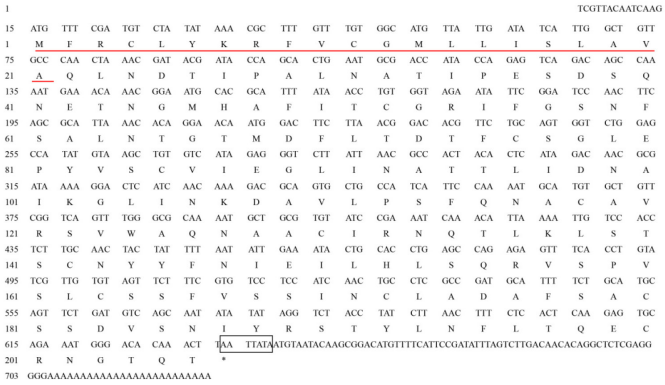

Figure 3. Nucleotide and deduced amino acid sequence of hic22 cDNA. The putative signal peptide is underlined. The putative polyadenylation signal (AATTATA) is boxed. The cDNA sequence of hic22 has been submitted to GenBank (Accession No. KR534871).

Figure 4. Secondary structure prediction of hic22. Based on the protein sequence of hic22, the secondary structure was predicted by Phyre2. The amino acids are colored according to the physiochemical properties of the side chains. The regions adopting putative β-sheet conformations are indicated by blue arrows. Degree of confidence = 0.9 is indicated by a rainbow-colored gradient.

Tissue expression and *in situ* hybridization

The results of qRT-PCR in seven *H. cumingii* tissues show the specificity of the expression of hic22 in the mantle, and that the expression occurred mainly in the pallial portion (Figure 5). The location and distribution of hic22 in the mantle was investigated by *in situ* hybridization. The DIG-labeled probes indicated that hic22 was strongly expressed in the mantle pallial portion (Figure 6).

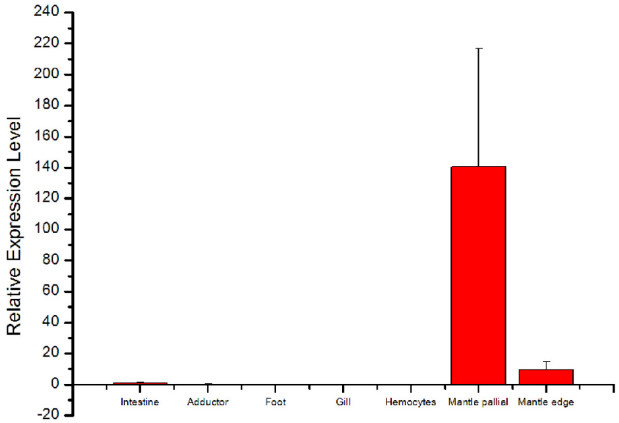

Figure 5. Tissue-specific expression of hic22 by qRT-PCR.

Figure 6. *In situ* hybridization of hic22 expression in the mantle of *Hyriopsis cumingii*. (IF, inner fold; MF, middle fold; OF, outer fold).

Analysis of hic22 expression during pearl sac formation and early development

Analysis of the data obtained from the pearl-nucleus-inserting experiment indicated that the expression of hic22 remained low between days 3 and 12 post-implantation/insertion. The hic22 expression was observed to increase during the pearl sac formation between days 12 and 77, with a peak observed at day 77 (Figure 7).

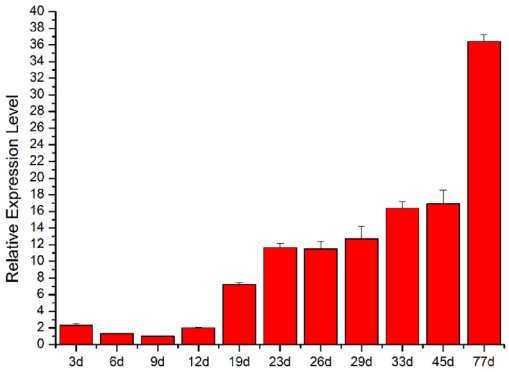

Figure 7. Relative expression of hic22 in the pearl sac during the early stages of pearl formation after implantation.

DISCUSSION

Nacre formation by *H. cumingii* is a complex process controlled by multiple matrix proteins. These proteins reportedly play an important role in the biomineralization of the nacreous layer. However, few of these proteins have been identified and characterized. Nacrein is known to accelerate the growth of the prismatic-shaped crystal (Han et al., 2010), whereas silkmapin is believed to provide the nucleation sites for the formation of the nacreous and prismatic layers in the shell (Liu et al., 2015). In this study, a novel matrix protein, hic22, was separated from the nacreous layer, and the complete cDNA encoding hic22 was obtained. BLASTp analysis indicated that hic22 was not homologous with known proteins. Following the removal of the signal peptide, the isoelectric point of hic22 was estimated to be 6.03, indicating that hic22 is a weak-acid matrix protein. The protein is composed of 186 amino acid residues; although the protein composed of all 20 of amino acids, it had a high proportion of serine (11.83%), asparagine (9.68%), leucine (9.19%), threonine (8.6%), and alanine (8.6%).

The secondary protein structure was mainly composed of α-helices (68%), as predicated by Phyre2. It is worth noting that α-helices were continuous and divided into two regions by two β-sheet regions. The α-helix regions resembled two arms that were in contact with the outside environment. The amino acid residues asparagine and cysteine were located on the two arms. Therefore, we could theorize that asparagine residues act as calcium binding sites, whereas the cysteine functioned as the protein interaction sites.

The mantle is the most active factor in shell formation; the edge of the mantle plays a central role in the formation of the corneous and prismatic layers, whereas the mantle center is responsible for the nacreous layer formation (Takeuchi and Endo, 2006; Inoue et al., 2010). Owing to the narrow prismatic layer and the fact that it is covered by the nacreous layer in *H. cumingii*, the mantle pallial is often thought to be involved in the formation of the nacreous

layer. In this study, hic22 is specifically expressed in the mantle, chiefly in the pallial region. *In situ* hybridization further confirmed that hic22 was chiefly expressed in the dorsal epithelial cells of the mantle pallial. These results indicated that hic22 is a special matrix protein involved in the formation of the nacreous layer.

Moreover, hic22 was not highly expressed in the pearl sacs from days 1 to 12 post-implantation; this period was followed by significant expression between day 19 and day 77. The pearl formation process is believed to involve two phases. In the first phase, the pearl sac wraps around the nucleus following implantation and calcium carbonate ($CaCO_3$) is irregularly deposited on the bare nucleus. In the second phase, $CaCO_3$ is regularly deposited on the nucleus to form the mature nacreous layer (Liu et al., 2012). Therefore, it can be supposed that the low expression level of hic22 in the pearl sac during the early stages (between days 1 and 12) might be attributed to the irregular calcium carbonate deposition, whereas the expression of hic22 increased significantly during, and after, the formation of the first nacreous layer. These results indicated that hic22 plays an important role in the formation of the nacreous layer of pearls.

In this study, the function of hic22 was mainly researched on a genetic level. The results showed that hic22 played a role in the nacreous layer formation by controlling the regular deposition of $CaCO_3$. Further studies should focus on the expression of the fusion protein in order to explore its role in guiding crystal growth and morphology, as well as its regulatory role in the nacreous layer formation.

Conflicts of interest

The authors declare no conflict of interest.

ACKNOWLEDGMENTS

Research supported by grants provided by the National Science and Technology Support program (#2012BAD26B04), the Shanghai Collaborative Innovation Center for Aquatic Animal Genetics and Breeding (#13DZ228050031272657), and the National Natural Science Foundation of China (#ZF1206).

REFERENCES

Addadi L, Joester D, Nudelman F and Weiner S (2006). Mollusk shell formation: a sour ce of new concepts for understanding biomineralization processes. *Chemistry* 12: 980-987. http://dx.doi.org/10.1002/chem.200500980

Alivisatos AP (2000). Biomineralization. Naturally aligned nanocrystals. *Science* 289: 736-737. http://dx.doi.org/10.1126/science.289.5480.736

Bai Z, Wang G, Liu X and Li J (2014). The status and development trend of freshwater pearl seed industry in China. *Shanghai Hai Yang Da Xue Xue Bao* 23: 874-881.

Han J, Li W, Shi Z, Hao Y, et al. (2010). Nacrein gene clone, protein extraction and its effect on crystal growth in *Hyriopsis cumingiilea. Biotech Bull* 12: 137-141.

Inoue N, Ishibashi R, Ishikawa T, Atsumi T, et al. (2010). Gene expression patterns and pearl formation in the Japanese pearl oyster (*Pinctada fucata*): A comparison of gene expression patterns between the pearl sac and mantle tissues. *Aquaculture* 308: S68-S74. http://dx.doi.org/10.1016/j.aquaculture.2010.06.036

Kono M, Hayashi N and Samata T (2000). Molecular mechanism of the nacreous layer formation in Pinctada maxima. *Biochem. Biophys. Res. Commun.* 269: 213-218. http://dx.doi.org/10.1006/bbrc.2000.2274

Lin JY, Ma KY, Bai ZY and Li JL (2013). Molecular cloning and characterization of perlucin from the freshwater pearl mussel, *Hyriopsis cumingii. Gene* 526: 210-216. http://dx.doi.org/10.1016/j.gene.2013.05.029

Liu X, Dong S, Jin C, Bai Z, et al. (2015). Silkmapin of *Hyriopsis cumingii*, a novel silk-like shell matrix protein involved in nacre formation. *Gene* 555: 217-222. http://dx.doi.org/10.1016/j.gene.2014.11.006

Liu X and Li J (2015). Formation of the prismatic layer in the freshwater bivalve Hyriopsis curninqii: the feedback of crystal growth on organic matrix. *Acta Zool.* 96: 30-36. http://dx.doi.org/10.1111/azo.12048

Liu X, Li J, Xiang L, Sun J, et al. (2012). The role of matrix proteins in the control of nacreous layer deposition during pearl formation. *Proc. Biol. Sci.* 279: 1000-1007. http://dx.doi.org/10.1098/rspb.2011.1661

Ma Y, Gao Y and Feng Q (2011). Characterization of organic matrix extracted from fresh water pearls. *Mater. Sci. Eng. C* 31: 1338-1342. http://dx.doi.org/10.1016/j.msec.2011.04.016

Ma Y, Qiao L and Feng Q (2012). *In-vitro* study on calcium carbonate crystal growth mediated by organic matrix extracted from fresh water pearls. *Mater. Sci. Eng. C* 32: 1963-1970. http://dx.doi.org/10.1016/j.msec.2012.05.030

Ma Y, Berland S, Andrieu JP, Feng Q, et al. (2013). What is the difference in organic matrix of aragonite vs. vaterite polymorph in natural shell and pearl? Study of the pearl-forming freshwater bivalve mollusc *Hyriopsis cumingii. Mater. Sci. Eng. C* 33: 1521-1529. http://dx.doi.org/10.1016/j.msec.2012.12.057

Ma YF, Gao YH and Feng QL (2010). Effects of pH and temperature on CaCO3 crystallization in aqueous solution with water soluble matrix of pearls. *J. Cryst. Growth* 312: 3165-3170. http://dx.doi.org/10.1016/j.jcrysgro.2010.07.053

Miyashita T, Takagi R, Okushima M, Nakano S, et al. (2000). Complementary DNA cloning and characterization of pearlin, a new class of matrix protein in the nacreous layer of oyster pearls. *Mar. Biotechnol.* 2: 409-418.

Natoli A, Wiens M, Schröder HC, Stifanic M, et al. (2010). Bio-vaterite formation by glycoproteins from freshwater pearls. *Micron* 41: 359-366. http://dx.doi.org/10.1016/j.micron.2010.01.002

Norizuki M and Samata T (2008). Distribution and function of the nacrein-related proteins inferred from structural analysis. *Mar. Biotechnol. (NY)* 10: 234-241. http://dx.doi.org/10.1007/s10126-007-9061-x

Sarikaya M and Aksay IA (1992). Nacre of abalone shell: a natural multifunctional nanolaminated ceramic-polymer composite material. *Results Probl. Cell Differ.* 19: 1-26. http://dx.doi.org/10.1007/978-3-540-47207-0_1

Takeuchi T and Endo K (2006). Biphasic and dually coordinated expression of the genes encoding major shell matrix proteins in the pearl oyster *Pinctada fucata. Mar. Biotechnol.* 8: 52-61. http://dx.doi.org/10.1007/s10126-005-5037-x

Veis A (1981). The chemistry and biology of mineralized connective tissues. Elsevier/North-Holland Press, New York.

Zheng HF, Bai ZY, Lin JY, Wang GL, et al. (2015). Characterization and functional analysis of a chitin synthase gene (HcCS1) identified from the freshwater pearlmussel *Hyriopsis cumingii. Genet. Mol. Res.* 14: 19264-19274. http://dx.doi.org/10.4238/2015.December.29.36